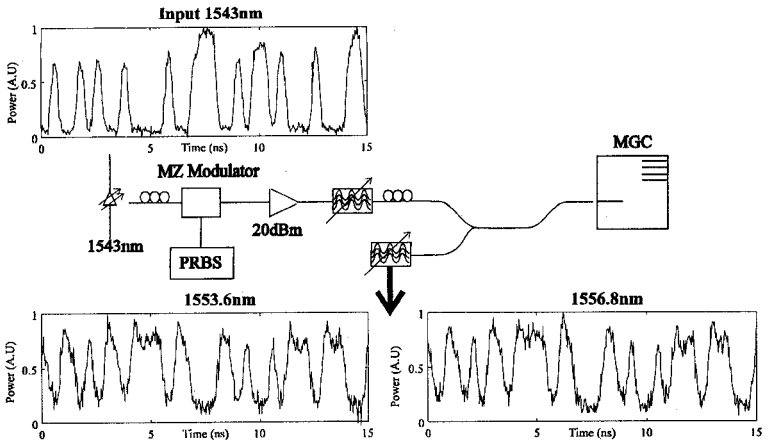

CThZ6 Fig. 2. Demonstration of 2.488-Gbit/s wavelength conversion using the MGC laser in one possible configuration allowing conversion to all four MGC lasing wavelengths. Converted patterns for two of the four MGC lasing wavelengths are shown.

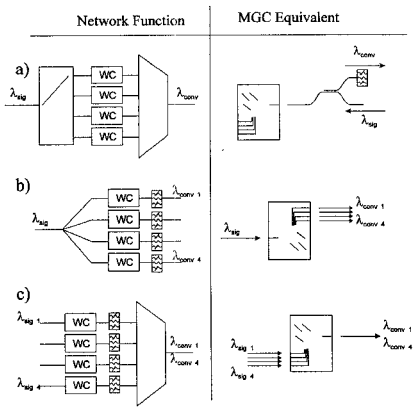

CThZ6 Fig. 3. Novel networking configurations that have been performed by the MGC laser. WC: wavelength converter. (a) Multichannel wavelength conversion as demonstrated in Fig. 2. (b) 1 × 4 broadcast and select wavelength conversion. (c) simultaneous wavelength conversion and multiplexing.

CThAA 4:30 pm–6:00 pm
Room 220–226

Optical Routing and Processing

Bahram Jalali, *University of California, Los Angeles, Presider*

CThAA1 4:30 pm

Out-of-plane vertical torsion mirror for optical scanner and chopper applications

G.D. Su, S.S. Lee, M.C. Wu, *UCLA, Electrical Engineering Department, 66-147D Engineering IV, 405 Hilgard Avenue, Los Angeles, California 90095-1594; E-mail: wu@icsl.ucla.edu*

Optical scanners are widely used in scientific and industrial applications ranging from laser imaging to printers and scanning displays. The micromachining technology is very attractive to miniaturize the scanners. Previously, optical scanners were realized by both bulk and surface-micromachining technology.[1–3] Surface-micromachined optical scanners with out-of-plane mirrors are particularly interesting because they can be integrated with other micromechanical and/or optoelectronic devices. However, the angles of current surface-micromachined scanners are limited by the displacement of in-plane actuators such as comb drive and bimorph microactuators. Torsion mirrors with gap-closing actuators, on the other hand, have larger rotation angles. In this paper, we propose an out-of-plane vertical torsion mirror that can be used as a scanner or a microchopper. This device is compact and lightweight and can be mass produced at a potentially low cost.

The scanning electron micrograph (SEM) of the vertical torsion mirror is shown in Fig. 1. The fabrication of the platform is done at the MEMS Technology Application Center at North Carolina (MCNC). The scanner consists of a vertical torsion mirror and a fixed back electrode. The torsion mirror is suspended by a vertical polysilicon frame and is designed to rotate up to 20° toward the back-electrode plate. The back-electrode plate is integrated with a scratch drive actuator array for self-assembly. The tips extruded from the side latch (Fig. 1) serve as a mechanical stop to prevent the torsion mirror from contacting the back electrode. The principle of operation is illustrated in Fig. 2. The mirror is 300 μm wide, 250 μm tall, and 1.5 μm thick. The torsion beam is 912 μm long, 2 μm wide, and 1.5 μm thick. The scan angle versus dc bias voltage and its frequency response are plotted in Figs. 3(a) and 3(b), respectively. The torsion mirror has a pull-in voltage of 136.5 V and a release voltage of 115 V. The resonant frequency is measured to be 0.5 kHz. The torsion mirror can operate in either small-signal or large-signal regime. For small-signal operation, the mirror scans up to 20° and can be used as a scanner. When the peak bias voltage exceeds 136.5 V, the mirror operates in bistable mode and can be used as an optical switch or chopper. For switch application, the switching time is measured to be <1 ms. It can also be used as a chopper if the deflected light is made to miss the aperture of the next optical element, which has the same effect as blocking the light.

In summary, a novel surface-micromachined, out-of-plane vertical torsion mirror has been successfully demonstrated. An optical scan range of 40° and a resonant fre-

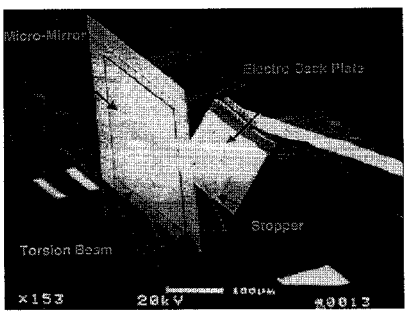

CThAA1 Fig. 1. Scanning electron micrograph of the vertical torsion mirror.

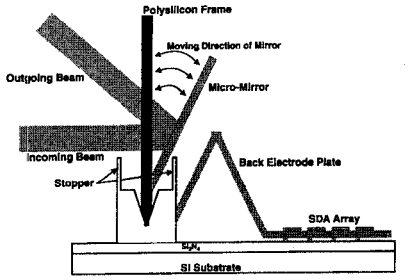

CThAA1 Fig. 2. Schematic diagram illustrating the operation of the vertical torsion mirror.

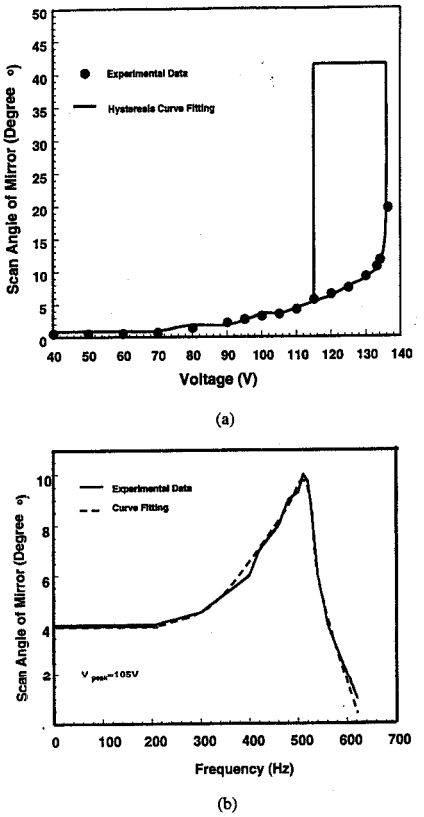

CThAA1 Fig. 3. (a) Scan angle versus applied dc bias voltage. (b) Frequency response of the vertical torsion mirrors.

Thursday, May 7

quency of 0.5 kHz have been achieved. Its applications include optical scanners, switches, and on-chip optical choppers for monolithic micro-optical instruments.

This project is supported in part by DARPA under DABT63-95C-0050.

1. M.-H. Kiang, O. Solgaard, R.S. Muller, K.Y. Lau, "High-precision silicon micromachined micromirrors for laser beam scanning and positioning," in *Solid-State Sensor and Actuator Workshop, Late News Paper, Hilton Head Island, S.C.* June 2–6, 1996.
2. M.E. Motamedi, S. Park, A. Wang, M. Dadkhah, A.P. Andrews, H.O. Marcy, M. Khoshnevisan, A.E. Chiou, R.J. Huhn, C.F. Sell, J.G. Smits, Opt. Eng. **36,** 1346–1353 (1997).
3. M. Ikeda, H. Goto, H. Totani, M. Sakata, T. Yada, "Two-dimensional miniature optical scanning sensor with silicon micromachined scanning mirror," in *Miniaturized Systems With Micro-Optics and Micromechanics II,* Proc. SPIE **3008,** 111–122 (1997).
4. S.-S. Lee, M.C. Wu, "Surface-micromachined vertical torsion mirror switches," in *International Conference on Optical MEMS and Their Applications,* Nara, Japan, November 18–21, 1997 (MOEMS 1997).

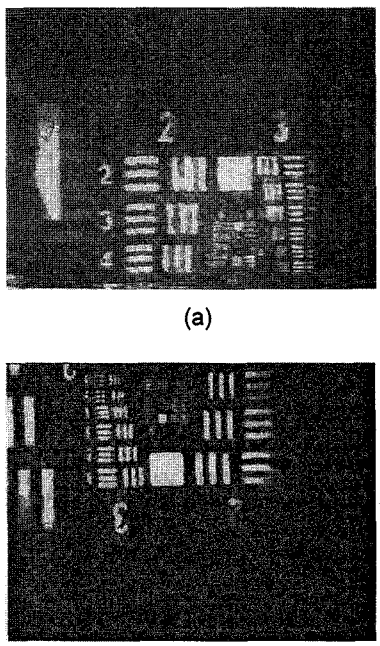

CThAA2 **Fig. 2.** Experimental setup for nonmechanical image rotation.

CThAA2 4:45 pm

Nonmechanical image rotation with an acousto-optic dove prism

Eung Gi Paek, Joon Y. Choe,* Tae K. Oh,* John H. Hong,** Tallis Y. Chang,** *National Institute of Standards and Technology, Gaithersburg, Maryland 20899*

Image rotation is important for various applications such as rotational invariant pattern recognition, computer graphics, and beam steering of phased-array antennas. Most of the techniques rely on the mechanical rotation of a dove prism as shown in Fig. 1(a). However, such a mechanical process is slow and unreliable.

We propose a new image rotation method that is both nonmechanical and programmable to permit rotation of an image to an arbitrary angle in a controllable manner. It is based on an analysis of a conventional dove prism. As illustrated in Fig. 1(b), a dove prism can be divided into three parts: the first part is a wedge prism to direct the incident beam to the bottom (or top) of the second part, which functions as a mirror to reflect the incoming light. The third part is another wedge prism to redirect the beam along the original direction. These three parts rotate together.

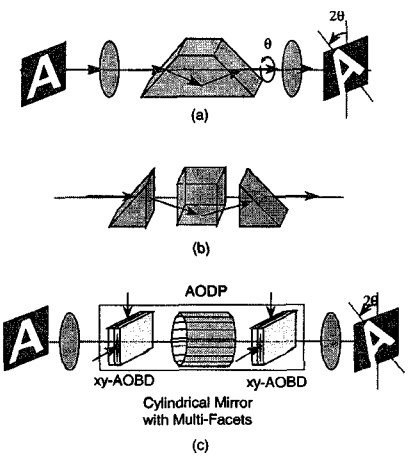

CThAA2 **Fig. 1.** Image rotation methods: (a) conventional mechanical method using a dove prism, (b) three parts of a dove prism, and (c) the proposed nonmechanical image rotation using an AODP (acousto-optic dove prism).

Our approach for nonmechanical image rotation is shown in Fig. 1(c). Each of the rotating wedges (the first and third parts of a dove prism) is replaced by an *xy* acousto-optic beam deflector (*xy*-AOBD). The *xy*-AOBD consists of a pair of crossed AOBDs sandwiched together with transducers along orthogonal directions. By adjusting the frequencies of acoustic signals applied to the two AOBDs, beam direction can be changed along arbitrary directions, just as a wedge does.

The reflecting mirror (second part) is replaced by a circular cylindrical mirror to avoid the need for rotation. To prevent unwanted distortion due to the curvature of the circular mirror surface, the cylindrical mirror is discretized to multiple facets. Also, incoming light is focused to have a minimum size on the mirror surface. In this way, an image can be rotated fast (on the order of microseconds) to an arbitrary angle in a programmable manner, without requiring any moving parts. Since the concept is based on the conventional dove prism, the name acousto-optic dove prism (AODP) has been proposed.

Figure 2 illustrates an experimental result obtained with our optical system. Using the two mirrors at a right angle, the two images are rotated 180° (twice the angle between the two mirrors). A real-time image rotation was achieved within 10 μs with a 6-mm aperture in front of the AOBDs. Also, rotations to other angles have been confirmed separately.

This work was supported by the Office of Naval Research (ONR) under contract number NC0014-97-F-0021.

*NSWC Dahlgren Division, 17320 Dahlgren, Virginia 22448-5100
**Rockwell International Science Center, Thousand Oaks, California 91360

1. E.G. Paek, J.Y. Choe, T.K. Oh, T.Y. Chang, J.H. Hong, Opt. Lett. **22,** 1195 (1997).

CThAA3 (Invited) 5:00 pm

Silica-based planar optical waveguide devices by TEOS/O_3 APCVD method

Mitsuhiro Kitamura, Naoki Kitamura, Masataka Itoh, *Opto-Electronics and High Frequency Device Research Laboratories, NEC Corporation, 4-1-1 Miyazaki, Miyamae-ku, Kawasaki, Kanagawa 216, Japan; E-mail: m-kita@oel.cl.nec.co.jp*

The technology of silica optical waveguides on Si substrate is attractive not only for passive planar lightwave circuits (PLCs) but also for hybrid integration of functional devices for optical communications and interconnections. Various devices such as the wavelength-division-multiplexing (WDM) transceiver module for optical subscriber systems and high-speed transmitter and receiver modules have been reported with this hybrid integration technology.[1] For the hybrid integration with PLC platform, it is highly desirable that V grooves for optical fiber assembly and signal electrode wiring can be easily formed with high-quality optical circuits. For this purpose, we adopted tetraethoxysilane (TEOS)/O_3 atmospheric pressure chemical vapor deposition (APCVD) method, where process temperature is drastically lowered so that metals for various patterned etching masks and electrical wiring can be formed before silica film deposition. With this feature of APCVD, novel optical functional devices with hybrid integration can be created. In this paper, we describe hybrid integrated optical waveguide devices with a special emphasis on the advantage of TEOS/O_3 APCVD method.

For APCVD, TEOS was employed as a precursor. Because TEOS is decomposed with O_3 at relatively low temperatures, high-quality thick silica films can be formed with low stress. Thick (~30 μm) silica glass layers have been deposited at temperatures as low as 450°C. The cladding layer and core layer consist of germanium-phosphorus-doped silica glass (GPSG). The difference in refractive index between the core layer and cladding layer can be controlled with tetramethoxygermanium (TMG) flow rate. Deposited films are annealed at 850°C. As low as 0.05-dB/cm optical propagation loss is routinely obtained for the waveguides with typically 6 × 6 μm cross section and 0.5% refractive-index difference. A very low birefringence of 3×10^{-5} has also been confirmed. The low deposition and annealing temperature enables metal layers, such as WSi, employed as masks for fiber guides and electrical wiring inside the silica layer, which offers the possibility of novel hybrid-integrated devices.